A Digital Elevation Model of the Barnes Ice-Cap Derived from Landsat MSS Data

G. D. Lodwick
S. H. Paine
Division of Surveying Engineering, The University of Calgary,
Calgary, Alberta T2N 1N4, Canada

ABSTRACT: This research study sought to investigate the feasibility of applying Landsat imagery to topographic mapping; in particular, to look at the possibility of deriving quantitative terrain data (slope and aspect information) from the variation in Landsat video response levels. A segment (approximately 34 by 47 km) of two different images of the Barnes Ice-Cap on Baffin Island was investigated. After enhancement of the data, the images were rectified using polynomial modeling and spatial resection to ground control. Resampling was carried out so that data from each image could be overlain directly. Twenty sites were used as training samples to relate slope and aspect information to video response levels. Experimentation was carried out with three different reflectance models, two of which used training samples, and the other which used general information obtained from the histograms of video data for the image segments and estimated terrain information. Slopes for each resampled 50 m square data element were calculated in the directions of sun azimuth for both images, and the absolute orientation of each surface element was calculated from the two pieces of information. This provided height differences in X and Y (the East and North directions). For a 22 km square block, a parametric least-squares adjustment was carried out to nine control points using the redundant information from the network of X and Y values. The general form of the surface estimated by this procedure agrees well with the actual mapped surface. Altogether, the study has shown that substantial topographic detail can be derived from Landsat data, which could have useful practical applications.

INTRODUCTION

INFORMATION concerning terrain topography is contained in Landsat imagery. This can be seen by inspection of images which include areas of relief differences. The effect of variations in slope and aspect is to modify the spectral signatures of the surface cover. In areas of sunfacing slopes, the response values in all bands will be upshifted towards the brighter end of the response scale; conversely, on awayfacing slopes the response values will be downshifted towards the darker end of the response scale. Traditionally, techniques such as ratioing are used to reduce this topographic effect.

To eliminate the effects of slope and aspect, so as to produce more refined spectral signatures, methods have been reported to directly adjust the response values. Malila *et al.* (1977), for example, used the Suits (1971) model to predict for individual images the reflectance of a pine forest under various slope and aspect conditions. Driscoll *et al.* (1974), working with the four original bands, constructed a linear model to describe reflectance variations with slope, and reported improvement in classification of coniferous forests as a result. Holben and Justice (1979) and Justice and Holben (1979) developed radiance simulation models to represent radiances from flat surfaces with a nadir pointing sensor, in order to reduce sun angle differences between multitemporal data sets. Holben and Justice (1980) further determined that spectral band ratioing could reduce the topographic effect by as much as 83 percent.

The fact that this topographic effect is present in Landsat imagery offers the alternative option, *viz.*, to enhance, rather than remove it. Such an approach was reported in research by Donker and Meijerink (1977). They investigated digital processing of Landsat imagery to produce a maximum impression of terrain ruggedness, using illumination criteria defined by Brassel (1974). Using a principal component (PC) transformation, they concluded that "one principal component, in general the first one, will represent the variation in illumination of the scene." This is consistent with the views expressed by Kauth and Thomas (1976) who named the four principal components, respectively, "brightness," "green-stuff," "yellow-stuff," and "non-such." Malila *et al.* (1977) have drawn similar conclusions as to "brightness" and "greenness" in their attempts at multispectral analysis through modeling and simulation.

In order to differentiate the brightness effects in PC1 scores, Lodwick (1979) designed a simple mathematical model to give, for each site, a value based on the illumination geometry. From a statistical

PHOTOGRAMMETRIC ENGINEERING AND REMOTE SENSING,
Vol. 51, No. 12, December 1985, pp. 1937-1944.

0099-1112/85/5112-1937$02.25/0

analysis of a number of images for a section of the Tamworth (Australia) scene, he concluded that, in rugged areas for lower sun angles (such as in winter images), the effect of topography on response levels for scores can be so significant as to mask the intrinsic differences between the ground cover classes themselves.

The above work shows that Landsat data contain information on topography. Also, that the imagery can be enhanced (for example by principal components analysis) to concentrate this information. This leads to the question as to whether quantitative detail on topography can be extracted from Landsat data.

Using multiple imagery from the Tamworth scene and the quantitative model derived earlier, Lodwick (1981a) was able to show a high correlation between score and site slope/aspect, and from this relationship topographic profiles in areas of similar terrain were accurately predicted. In order to be able to utilize such a technique however, the area under consideration needs to be composed of a single ground cover category only. Otherwise, variations in scores may refer to intrinsic surface differences, rather than to brightness differences caused by differential lighting effects. Also, to extend the method to produce three-dimensional (i.e., X,Y,Z) information, at least two images are required to give at least two look angles. The whole approach has been neatly described by Kratky (personal communication) as the reverse of perspective shading. Here there is a perfectly shaded image, and through the use of two images (giving different perspectives) the primary three-dimensional surface can be derived.

The aim of this research was to attempt to apply and extend these emergent techniques to a suitable target. An immediate potential application was to ice-caps, first of all because they have a relatively homogeneous surface, and secondly because of difficulties in mapping them by conventional means. The computer system used in the study has been described in Lodwick (1981b). In the course of this work, the system, which had been developed at the University of New South Wales, was transferred onto the Honeywell 66/80 computer at The University of Calgary.

IMAGE SELECTION

A listing of Landsat imagery, covering the Barnes Ice-Cap, on Baffin Island, Canada revealed a total of 44 Landsat-1 and Landsat-2 images available with less than 20 percent cloud cover and of at least minimum quality 'Fair' in all four bands. These images came from four tracks (26-010, 27-010, 28-010, 29-010) and indicate the extent of image redundancy caused by the reduced separation of the satellite track at high latitudes. This redundancy substantially compensates for the higher image rejection rate, caused by greater cloud coverage and six months of reduced lighting conditions, in the arctic regions. A number of images were considered possible for the study but in the end two were selected, one from Landsat 1, taken 23 July 1976, and one from Landsat 2, taken 9 October 1980. These dates were chosen to give as high and low a sun angle as possible, as well as a maximum difference in sun azimuth. The sun elevation and azimuth for July are 38 and 153 degrees respectively, and for October, 11 and 175 degrees respectively. The Landsat image for band 7 for the study area is displayed in Figure 1. Multispectral Scanner (MSS) digital data on computer compatible tapes were obtained from the Canada Centre for Remote Sensing.

DATA DISPLAY AND ENHANCEMENT

The 600 by 600 pixel (around 34 by 47 km) segment selected for detailed study is situated at the northwest tip of the Barnes Ice-Cap. Its position is marked on the July image (Figure 1). Apart from being located on both images (which are from different tracks), the end of the ice-cap offered a range of slopes and aspects which would be helpful in the analysis. Another important advantage was that this section included much of the glacier perimeter, which was useful for control point selection in image rectification.

For the July image, histograms of the response levels revealed that saturation has occurred for bands 4, 5, and 6, where a large proportion of the pixels have maximum values. Also, the form of the distributions in those bands is multimodel. The various nodes of response values correspond to the snow-covered ice-cap, to snow-free areas of tundra, and to darker patches of melt water on parts of the glacier surface. For the October image the distribution is symmetrical because of snow which is now covering the tundra, and the ice-cap is completely frozen. More importantly, the data show that for this image the response levels are well below saturation.

VIDEO DATA CORRECTION

Detailed investigation of Landsat data requires analysis of a four-band data-set. Principal Components Analysis (PCA) is useful for this purpose because it can usually reduce the spatial complexity of multivariate problems (Davis, 1973). With Landsat data, because of the high correlation between the original bands, the first (PC1) and second principal components (PC2) typically account for more than 95 percent of the total variance in the original data. Thus, the original spectral position of a particular data element can be defined in terms of a vector in two dimensions with negligible loss of information, and this can be compared to those of other elements.

For the October image the principal components were calculated. Inspection of the transformation showed that PC1 contributes over 95 percent of the variance, PC2 over two percent, and PC3 and PC4

each around one percent. Thus, all the information can be displayed by means of a single new variable, with little loss of information. The form of the transformation showed PC1 to be simply the negative sum of the original band values, whereas PC2 is the difference between the response levels in the visible bands and the infrared bands. These correspond to what are generally called the "brightness" and "greenness" vectors. Thus, brightness information for the ice-cap should be contained in PC1 scores, whereas PC2 scores should contain information which is specifically surface-cover related.

For July, principal components could not be calculated, because the form of the distribution is not symmetrical for all bands, and so summarizing the data in terms of means and variances would not be valid. Thus, the analysis proceeded on the basis of using the PC1 data sets for October and band 7 alone for July.

IMAGE RECTIFICATION

The method of rectification involved spatial resection to ground control points using polynomials. Image rectification using polynomials has been discussed by Derouchie and Forrest (1974) and Wong (1975). The particular method used in this system has been outlined by Lodwick (1978) and Trinder and Smith (1979). With this approach certain known geometric errors need to be taken into account before rectification. These are the swath discontinuous errors (sensor delay and Earth rotation). The swath continuous errors (e.g., non-linear mirror velocity) and the global continuous errors (e.g., roll, pitch, yaw) are fully accommodated by the modeling procedure.

Altogether 21 points were identified for control using shade prints and character prints. The control points were natural features situated around the margin of the ice-cap. Some were chosen on prominent tongues of glacier ice which extended onto the snow-covered tundra, whereas others were lineaments or gullies whose positions could be determined, even though they were covered by snow. For well-defined points, selection of position on the base cap to 100 m was possible, whereas in other cases discrepancies in selected position could be as much as 500 m. Obviously, this is an important aspect of work in areas such as this.

From experience with the research, because only around 1/20th of an image is involved and also because of the relative difficulty in positioning the control points (due to limited identifiability, the low accuracy of the base map, and the fact that the margins of the glacier used for control appear to have moved slightly since the preparation of the map), complete second-order polynomials were used in the research rather than the third-order ones used to resect whole images. This allows less twisting of the image to the control, so that unwarranted surface fluctuations due to inherent ground control point errors will be reduced.

The polynomial equations used for the modeling are

$$X = a_0 + a_1x + a_2x^2 + a_3y + a_4y^2 + a_5xy \quad (1)$$
$$Y = b_0 + b_1x + b_2x^2 + b_3y + b_4y^2 + b_5xy \quad (2)$$

where

X and Y are ground coordinates (East and North), x and y are pixel column and row coordinates, and a_0 to a_5, b_0 to b_5 are the transformation parameters.

The second-order polynomials given in Equations 1 and 2 are solved by a least-squares procedure, both ground and image coordinates being considered subject to error. Appropriate variances are assigned to the image coordinates according to the estimated accuracy of measurement, and to the ground coordinates according to the assigned map accuracies and estimated pointing errors. Because the computer program allows a selected proportion of the error to be allocated to the ground data, the adjusted ground control values are likely to be better approximations of the actual positions than the original estimates.

From previous experience it was clear that selection of ground control was the inhibiting factor in the accuracy of the adjustment, so the variance factors were set to distribute the larger proportion of the error into ground control. After careful analysis and reworking of the control point data in the October image, the RMS errors in the adjustments were 0.34 and 0.51 pixel for image column and row and 252 and 241 m in ground X and Y.

For the July image only 17 of the selected 21 control points could be identified. However, this is clearly enough to obtain a satisfactory solution. The final result was similar to the result for the October image, with adjustment RMS errors of 0.35 and 0.35 pixel for image column and row and 237 and 200 m in ground X and Y.

IMAGE RESAMPLING

Because the research aimed to integrate data from two images, direct comparison at the pixel level is required. The method used here was nearest-neighbor resampling which has been outlined by Bernstein and Ferneyhough (1975). It has the property of retaining the original video values rather than producing a transformed data set. It also has the advantage of minimizing computer overheads.

Both image segments were resampled, based on a 50-m grid. Overlaying the two data sets showed that, for readily identifiable ground points, the locations on the two segments agreed to better than one pixel position. This further justified the error distribution as selected for the image and ground control in the rectification process.

Once the parameters for the second-order poly-

nomials are obtained, the ground coordinates for all pixel centers can be calculated directly. Alternatively, the pixel centers can be calculated from ground coordinates by a reverse computation of Equations 1 and 2. One method is to use the Newton-Raphson technique of successive approximations (Burden *et al.* (1978) p. 34), as outlined in Trinder and Smith (1979).

In order to proceed with the investigation of reflectance models, training samples are required. For this purpose, a selection of 20 sample sites was chosen, of suitable slopes and aspects in relation to the sun azimuth. These topographic values were read from the base map but, in practice, could be obtained from field measurements. The slope values varied from less than one degree on sunfacing slopes to around 15 degrees on awayfacing slopes on the ice-cap margin. These are similar in magnitude to slope values estimated from a traverse on the base map (see Figure 1). Pixel centers corresponding to the selected ground positions were calculated, and the reflectance values for each sample site determined to be the mean of the set of 5 by 5 pixels surrounding the position determined by the above resampling.

ALTERNATIVE REFLECTANCE MODELS

Three possible reflectance models were considered, a theoretical model and two empirical models.

(a) First, according to Teillet *et al.* (1982) simplified Lambertian conditions relating the radiances to topography can be defined as

$$L_H = L_T \cos Z / \cos i \qquad (3)$$

where

L_H = radiance observed for a horizontal surface,
L_T = radiance observed on sloped terrain,
Z = solar zenith angle = incident angle for horizontal surface, and
i = incident angle with respect to surface normal.

From the training sample values, calculations were made of L_H, the radiance observed for a horizontal surface. These were calculated for the band 7 data for July and are plotted in Figure 2. As can be seen, rather than grouped closely around a mean value, the transformed data still have a significant variance and a clear linear regression component.

These calculations are based on the assumption that the ice surface is Lambertian. A Lambertian surface is one that scatters light equally in all directions. Looking at the results of the transformation as plotted in Figure 2, it can be seen that there is undercompensation at all slope angles. In other words, the original data recorded on the sunfacing slopes remain brighter than would be expected, and the data recorded on the awayfacing slopes remain darker than would be expected. This can be explained by the fact that an ice surface is more likely to exhibit specular reflection, with the majority of the energy being re-

FIG. 1. Landsat 1 image of the Barnes Ice-Cap taken 23 July 1976.

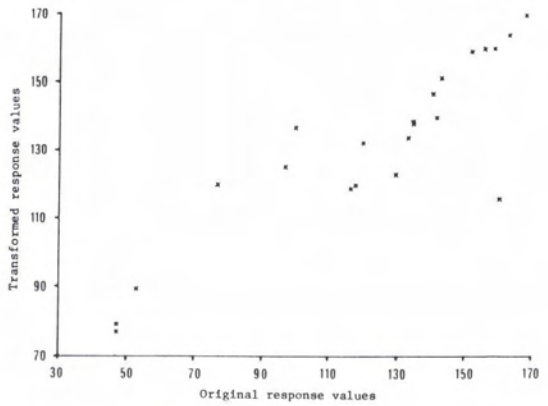

FIG. 2. Video response values for band 7 for the July image, corrected for Lambertian reflectance.

flected at an angle equal and opposite to the incident energy. Thus, it seems clear that, for an ice-cap, the reflectance conditions are non-Lambertian. Indeed, even in work done for pine forest cover types, Smith *et al.* (1980) found that the Lambertian assumption is only valid over a small range of incident angles.

(b) A second alternative is to look at the original data (as represented by the training samples) for both data sets and try to model the relationships directly, for example, by means of polynomial regression. The original data values showing video response levels versus slopes are plotted in Figures 3a and 4a. (Note that, for the July band 7 data, the response values have been transformed by subtracting 128 and dividing by 10 to give values of similar magnitude to the PC scores of October.) First-order and second-order curves were fitted to both sets of data, although only the first-order curves are plotted. For July the correlation coefficients were respectively 0.92 and 0.93, indicating a high degree of correlation between the two sets of data. For October, the correlation coefficients were respectively 0.85 and 0.86, also indicating very high correlations. These results suggest that, over the limited range of slopes involved in this work, there is a simple relationship between topography and reflectance.

As shown in Figure 5, once the slopes in the directions of sun azimuth are known, these can be converted into h_1 and h_2 values, or estimates of heights across each pixel. From these values, each pixel slope and orientation can be calculated, which allows derivation of the X and Y values, the height changes in the East and North directions. The values were calculated for a 440 by 440 pixel area covering a total of 22 by 22 km, centered in the North of the image segment shown in Figure 1. This embraced part of the ice-cap surface, where slopes radiated in several directions.

Using these models, X and Y values for all the pixels in the study area were calculated. The height components show symmetrical distributions with around two-thirds of the values within the range -25 to $+13$ m for X and -3 to $+4$ m for Y. Inspection of the base map suggests that the Y values are closely comparable to the actual values, whereas the X values appear to be much larger than expected values. One possible reason for this is that slope estimation is best in the directions of sun azimuth, which are 153 degrees and 176 degrees. On this basis it is expected that the values calculated in the North-South direction should conform more closely to the actual values than values calculated in the East-West direction.

Nevertheless, the implication is that there is a systematic error involved in the modeling which has produced this result. Clearly, the use of a simple linear model involving the training samples has not achieved the desired results.

(c) A third possibility is to dispense with the use of training samples altogether. Instead, the approach is to take the values of typical steep slopes in the study area in both the sunfacing and awayfacing directions. From the histograms of video response levels, values at the one percent level at either end of the histograms are selected and the slope values are plotted against the reflectance values. A straight line is plotted between these points and the equation of this line is taken to represent the relationship between slope and reflectance.

For July and October the values obtained were as follows:

	July (sun 153°)	Band 7 (1%)
Max slope (facing)	50 ft/1000m	−5.4
Max slope (away)	−100 ft/1000m	+10.3
	October (sun 175°)	Score 1 (1%)
Max slope (facing)	75 ft/1000m	−2.6
Max slope (away)	−100 ft/1000m	5.3

These points and the lines involved are also plotted in Figure 3b and 4b. Immediately it can be seen that, particularly for July, there are significant differences between the slopes of these lines and the slopes of the lines produced using the training samples. For July, it can be seen that the previous regression line is determined significantly by the training samples of high slopes. These were selected from the steepest areas obtainable on the ice-cap, *viz.*, the cliffs where the ice-cap calved into the ocean. It thus seems likely that problems encountered using the Lambertian model and the linear model using the training samples may well have been compounded by using unrepresentative slope data.

Using these new regression lines, X and Y values were calculated for all the pixels in the study area. The height components show symmetrical distributions with around two-thirds of the values within the range -3 to $+3$ m for X and -3 to 0 m for Y, which much more closely correspond to the actual values observed on the base map.

INTEGRATION OF A DIGITAL ELEVATION MODEL

From the above investigation, the third reflectance model was used in the integration procedure. A computer program was written to adjust the grid using a parametric least-squares adjustment technique. Because there was a limitation on the size of

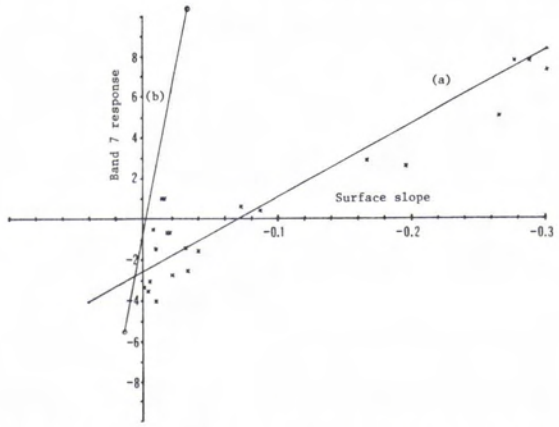

FIG. 3. Regression lines for July calculated (a) using the training samples and (b) using maximum slope data.

the matrix able to be inverted, the 50 by 50 m pixels were combined into composite 500 by 500 m pixels for adjustment. Thus, for the 22 by 22 km area, the total number of combined 500 by 500 m pixels is 44 in each direction. The adjustment for the whole surface was carried out using a weighted third-order surface fit to nine control points situated at the corners, the mid-points of the sides, and the center of the area.

The calculated surface is displayed as a contour diagram in Figure 6. This can be compared to the actual surface as displayed in Figure 7. A comparison of Figure 6 and Figure 7 reveals a general agreement as to the basic shape of the surface. This is a fall of the ice surface towards the North-West, with another fall towards the North-East. The predicted surface however appears to show the ice-cap as surging further to the North-West (compare the 3000-ft contours) than the surface given by the base map. It is possible that this disagreement could

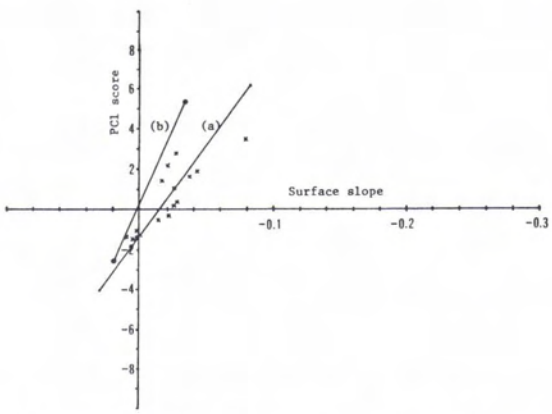

FIG. 4. Regression lines for October calculated (a) using the training samples and (b) using maximum slope data.

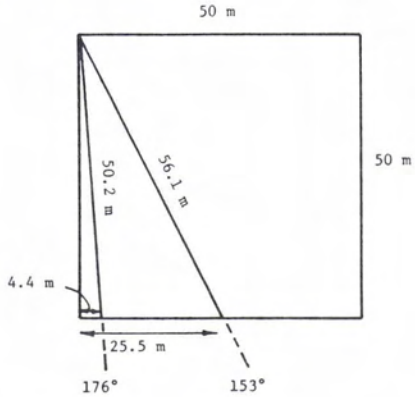

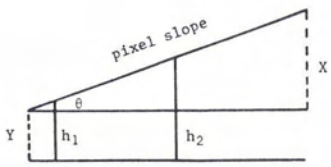

$h_1 = 50.2\ S_1$

$h_2 = 56.1\ S_2$

$\tan\theta = (h_2 - h_1) / (25.5 - 4.4)$

$X = 50 \tan\theta$

$Y = h_2 - 25.5 \tan\theta$

FIG. 5. Calculation of pixel geometry.

partly be the result of change of the surface of the ice-cap. The base maps were produced from aerial photography flown in 1961, and the ice surface is a mobile structure capable of substantial change with time. For example, inspection of the margins of the ice-cap clearly shows areas where there has been melt-back, and shrinking of the periphery. It is thus quite possible that the apparent surge shown on the predicted map is an actual feature resulting from melting and refreezing. Such activity has been reported on the Barnes Ice-Cap by Holdsworth (1977).

CONCLUSIONS

Altogether there are several conclusions that follow from this research.

First, even in Arctic areas there are sufficient images available to obtain a selection of cloud-free Landsat data. Because of the closer spacing of the satellite track (giving more overlap) at high latitudes, imagery can be selected from different paths, giving different acquisition times. This results in different sun azimuths, and thus a range of look directions. From experience with several images it seems clear that in summer saturation will occur in bands 4, 5, and 6, but band 7 will not be saturated. This will show good discrimination of ice surfaces

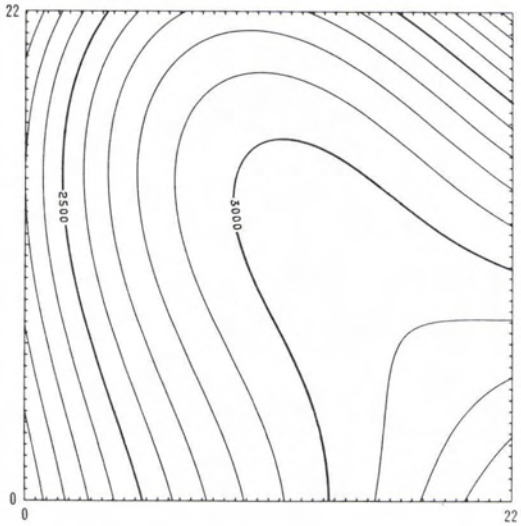

FIG. 6. Weighted third-order surface predicted by the linear model (scale in km, contours in feet).

through a large dynamic range of values. For non-summer imagery, where all four bands are not saturated, principal components analysis can be used to synthesize the multivariate data set. Effective analyses can be carried out by utilizing both types of information, separately or in combination.

Second, even in such difficult terrain as an ice-cap, sufficient identifiable features can be found to enable a suitable image rectification procedure to be carried out. In both image resections RMS adjustments in X and Y of between 200 and 250 m were obtained. These resulted from the use of second-order polynomials, which could be expected to give larger adjustments than third-order because they are less accommodating to control point errors. When the accuracy of the base map is taken into account, as well as the fact that in some places the margin of the ice-cap has clearly receded since the map was produced, the results can be seen to be quite good. As far as image comparison is concerned, RMS errors in the resection for column and row for both images varied around half a pixel. Comparison of identifiable features for both images within the resampled sections revealed positional accuracies to less than a single pixel. This confirmed the integrity of Landsat data, even where there is less certainty of ground control.

Third, an investigation of three alternative models to relate slope information to the video data revealed certain information:

(a) On the basis of work done for the July image, it appears that an ice-cap does not behave as a Lambertian surface. A theoretical correction of the video values using the known slopes of the training samples failed to bring the radiances to a common value as would be expected. In fact, the transformed data still contained a significant variance and linear regression component.

(b) Difficulties are encountered by using training samples and simple polynomial models, even though high correlations can be obtained. By implementing first-order regression models, histograms of height differences show height changes in X (the East direction) apparently much larger than exist. It seems likely that the difficulties occur because of problems in obtaining representative training data on the ice-cap surface.

(c) Application of a simple linear model, by utilizing typical maximum slopes on the ice-cap in the sun-facing and awayfacing directions and selecting reflectance values at the one percent level of the histograms of the video data, gives good results. Using the regression equations, histograms of X and Y height differences were produced which agreed broadly to the values observed on the base map.

Finally, from the use of multiple imaging and the simple model outlined in (c) above, it is possible to integrate different sets of Landsat data to determine terrain information for individual pixel elements 50 by 50 m in size. Using only nine control points, adjustment of X and Y data for all individual terrain elements using a weighted third-order surface fit enabled a digital elevation model of an area 22 by 22 km to be produced which is in good agreement with the surface of the ice-cap defined by the base map.

Thus, this study has developed a methodology which enables Landsat response values to be simply related to slope and aspect on ice-caps. What is necessary are first, Landsat data from two images which have the largest difference in sun azimuth obtainable, and second, an estimation of the maximum slopes existing on the ice cap. From this, by recti-

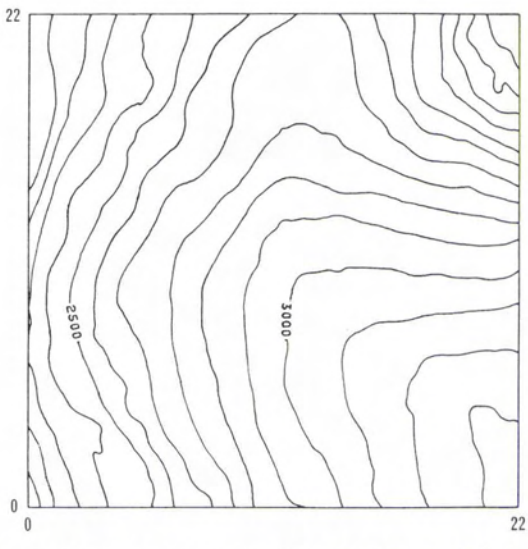

FIG. 7. Surface as given by the base map (scale in km, contours in feet).

fication of the imagery using polynomials and control points, height differences in X and Y for 50-m elements can be calculated and, by means of a parametric least squares adjustment, a three-dimensional digital elevation model produced.

ACKNOWLEDGMENTS

The work outlined in this paper was performed by the authors as part of EMR contracts OSO80-00357 and OST83-00180 carried out for the Topographical Survey Directorate, Surveys and Mapping Branch, Canadian Government, Department of Energy, Mines and Resources, Ottawa.

REFERENCES

Bernstein, R., and D. G. Ferneyhough, Jr., 1975. Digital image processing, *Photogrammetric Engineering*, Vol. 41, No. 12, pp. 1465-1476.

Brassel, K., 1974. A model for automatic hill-shading, *The American Cartographer*, Vol. 1, No. 1, pp. 15-27.

Burden, R. L., J. D. Faires, and A. C. Reynolds, 1978. *Numerical Analysis*, second edition, Wadsworth Inc., Boston, 598 p.

Davis, J. C., 1973. *Statistics and Data Analysis in Geology*, John Wiley and Sons Inc., New York, 550 p.

Derouchie, William F., and R. B. Forrest, 1974. Potential positioning accuracy of ERTS-1 MSS images, paper presented at the 1974 ACSM-ASP Convention, St. Louis, Missouri, March 1974.

Donker, N. H. W., and A. M. J. Meijerink, 1977. Digital processing of Landsat imagery to produce a maximum impression of terrain ruggedness, *International Institute for Aerial Survey and Earth Sciences (ITC) Journal*, Vol. 4, pp. 683-704.

Driscoll, R. S., R. E. Francis, J. A. Smith, and R. A. Mead, 1974. ERTS-1 data for classifying native plant communities—Central Colorado, *Proceedings of Ninth International Symposium on Remote Sensing of Environment*, University of Michigan, 1974, ERIM, Ann Arbor, Michigan, pp. 1195-1211.

Holben, B. N., and C. O. Justice, 1979. *Evaluation and modeling of the topographic effect on the spectral response from nadir pointing sensors*, TM 80305, NASA Goddard Space Flight Center, Greenbelt, Maryland.

———, 1980. *An examination of spectral band rationing to reduce the topographic effect on remotely sensed data*, TM 80640, NASA Goddard Space Flight Center, Greenbelt, Maryland.

Holdsworth, G., 1977. Surges in ice-sheets, *Nature*, Vol. 269, No. 5629, pp. 588-590.

Justice, C. O., and B. N. Holben, 1979. *Examination of Lambertian and non-Lambertian models for simulating the topographic effect on remotely sensed data*, TM 80557, NASA, Goddard Space Flight Center, Greenbelt, Maryland.

Kauth, R. J., and G. S. Thomas, 1976. The tasselled cap—a graphic description of the spectral-temporal development of agricultural crops as seen by Landsat, *Proceedings of Symposium on Machine Processing of Remotely Sensed Data*, Purdue University, LARS, West Lafayette, Indiana, pp. 4B-41, 4B-51.

Lodwick, G. D., 1978. Between scene registration accuracy in Landsat time sequencing, *Proceedings of the Twelfth International Symposium on Remote Sensing of Environment*, Manila, Philippines, ERIM, Ann Arbor, Michigan, pp. 1461-1470.

———, 1979. Measuring ecological changes in multitemporal Landsat data using principal components, *Proceedings of the Thirteenth International Symposium on Remote Sensing of Environment*, University of Michigan, ERIM, Ann Arbor, Michigan, pp. 1131-1141.

———, 1981a. Topographic mapping using Landsat data, *Proceedings of Fifteenth International Symposium on Remote Sensing of Environment*, University of Michigan, ERIM, Ann Arbor, Michigan, pp. 527-533.

———, 1981b. A computer system monitoring environmental changes in multitemporal Landsat data, *Canadian Journal of Remote Sensing*, Vol. 7, No. 1, pp. 24-33.

Malila, W. A., J. M. Gleason, and R. C. Cicone, 1977. Multispectral systems analysis through modeling and simulation, *Proceedings of Eleventh International Symposium on Remote Sensing of Environment*, University of Michigan, ERIM, Ann Arbor, Michigan, pp. 1319-1328.

Smith, J. A., T. L. Lin, and K. H. Rawson, 1980. The Lambertian assumption and Landsat data, *Photogrammetric Engineering and Remote Sensing*, Vol. 46, pp. 1183-1189.

Suits, G. H., 1971. The calculation of directional reflectance of a vegetative canopy, *Remote Sensing of Environment*, Vol. 2, No. 1, pp. 117-125.

Teillet, P. M., B. Guindon, and D. G. Goodenough, 1982. On the slope-aspect correction of multispectral scanner data, *Canadian Journal of Remote Sensing*, Vol. 8, No. 2, pp. 84-106.

Trinder, J. C., and C. J. H. Smith, 1979. Rectification of Landsat digital imagery, *Australian Journal of Geodesy, Photogrammetry and Surveying*, No. 30, pp. 15-30.

Wong, K. W., 1975. Geometric and cartographic accuracy of ERTS-1 imagery, *Photogrammetric Engineering and Remote Sensing*, Vol. 41, No. 5, pp. 621-635.

(Received 31 May 1983; accepted 9 October 1984; revised 25 June 1985)